JBC Papers in Press. Published on May 19, 2005 as Manuscript M500541200

$ICln_{159}$ Folds into a PH-Domain Like Structure: Interaction with Kinases and the Splicing-Factor LSm4

Johannes Fürst[1], Andreas Schedlbauer[2], Rosaria Gandini[1], Maria Lisa Garavaglia[3], Stefano Saino[3], Martin Gschwentner[1], Bettina Sarg[4], Herbert Lindner[4], Martin Jakab[2], Markus Ritter[1,5], Claudia Bazzini[3], Guido Botta[3], Giuliano Meyer[3], Georg Kontaxis[2], Ben C. Tilly[6], Robert Konrat[2] and Markus Paulmichl[1,3,*]

From the [1] Department of Physiology and Medical Physics, Innsbruck Medical University, Fritz-Pregl Strasse 3, A-6020 Innsbruck, Austria; [2] Institute of Theoretical Chemistry and Molecular Structural Biology, University of Vienna, Rennweg 52b, A-1030 Vienna, Austria; [3] Department of Biomolecular Sciences and Biotechnology, Università degli Studi di Milano, Via Celoria 26, I-20133 Milan, Italy; [4] Division of Clinical Biochemistry, Biozentrum, Innsbruck Medical University, Fritz-Pregl Strasse 3, A-6020 Innsbruck, Austria; [5] Institute of Physiology, Paracelsus Private Medical University, Stubergasse 21, A-5020 Salzburg, Austria; [6] Department of Biochemistry, Erasmus University Medical Center Rotterdam, Dr. Molewaterplein 50, 3015 GE Rotterdam, Netherlands

Running title: ICln structure and interactions

(*) Address correspondence to: Markus Paulmichl, Department of Physiology and Medical Physics, Innsbruck Medical University, Fritz-Pregl Strasse 3, A-6020 Innsbruck, Austria, or Department of Biomolecular Sciences and Biotechnology, Università degli Studi di Milano, Via Celoria 26, I-20133 Milan, Italy, Tel: +43 512-507-3756 or +39-02-5031-4947; FAX: +43-512-577656 or +39-02-5031-4948; E-mail: markus.paulmichl@ uibk.ac.at or markus.paulmichl@unimi.it

ICln is a multifunctional protein involved in regulatory mechanisms as different as membrane ion transport and RNA-splicing. The protein is water-soluble, and during regulatory volume decrease after cell swelling, it is able to migrate from the cytosol to the cell membrane. Purified, water soluble ICln is able to insert into lipid bilayers to form ion channels. Here we show that $ICln_{159}$, a truncated ICln mutant, which is also able to form ion channels in lipid bilayers, belongs to the PH-domain superfold family of proteins. The ICln PH-domain shows unusual properties as it lacks the electrostatic surface polarization seen in classical PH-domains. However, similar to many classical PH-domain-containing proteins, ICln interacts with PKC, and, in addition, interacts with PKA and PKGII but not PKGI. A major phosphorylation site for all three kinases is S45 within the ICln PH-domain. Furthermore, $ICln_{159}$ interacts with LSm4 - a protein involved in splicing and mRNA degradation - suggesting that the $ICln_{159}$ PH-domain may serve as protein-protein interaction platform.

ICln is a small (≈ 25kD), multifunctional protein involved in regulatory mechanisms as different as cell volume regulation and RNA-splicing (1,2). Proteins involved in more than one regulatory mechanisms were recently defined as 'connector hubs' (3), and play a pivotal role in cell function. Knock-out of such proteins is usually lethal. Accordingly, functional knock-out of the ICln protein in mouse or nematode is lethal in very early stages of development. No vital embryos can be obtained in either animal system (2,4), which suggests a key role of ICln in cell homeostasis.

ICln is water soluble (1) and resides primarily in the cytosol (5) where it forms heteromultimeric complexes with (i) Sm-proteins (6-9), (ii) the arginine methyltransferase PRMT5 (6-10) and (iii) cytoskeletal proteins like β-actin, erythrocyte protein 4.1 or the non-muscle isoform of the alkali myosin light chain (5,11-13). A fraction of ICln is associated with the cell membrane and interaction with the membrane protein integrin $\alpha_{IIb}\beta_3$ has recently been demonstrated (14).

During a hypotonic challenge ICln migrates from the cytosol towards the cell

membrane, suggesting a role for ICln in cell volume regulation (15). This regulatory mechanism is further substantiated by the finding that heterologous expression of ICln in *Xenopus laevis* oocytes is followed by the appearance of ion currents (1) resembling those elicited by swelling of mammalian cells (2,16). Furthermore, ICln-specific antibodies (5) or antisense oligodeoxynucleotides (17,18) leading to a specific knock-down of the ICln protein, impair regulatory-volume-decrease (RVD) in native cells. Conversely, over-expression of ICln in mammalian cells increases RVD-currents during a hypotonic challenge (2,19,20). In bacteria, overexpression of ICln leads to an improved tolerance to hypotonicity, an effect that can be reversed by the extracellular application of nucleotides (21,22). The extracellular effect of nucleotides was also shown for heterologous expression of ICln in oocytes, and the putative binding site for nucleotides was identified (1,23). The abovementioned findings point towards a channel function of ICln (1). The successful reconstitution of purified ICln in artificial lipid bilayers demonstrated that ICln can indeed form ion conducting channels whose selectivity depends on the lipid composition of the membrane (23-26).

Another well-documented function of ICln is its role in splicing. In the cytosol, ICln forms two separate complexes with splicing factors. One complex (6S) contains ICln and the Sm heteromers D1·D2, D3·B/B' and E·F·G. The other complex is composed of ICln, the arginine methyltransferase PRMT5, MEP-50 and Sm proteins, and is termed the methylosome. The current hypothesis on the role of ICln in the splicing process is, that ICln sequesters newly synthesized Sm proteins, directs these proteins to the methylosome, a protein complex that methylates Sm and possibly LSm-proteins, prior to the assembly of the cytoplasmic UsnRNA core particle by the SMN-complex (6-8).

For both functions of ICln, e.g. ion transport as well as splicing, the structure of ICln is of utmost importance to better understand - on a molecular level - the regulatory mechanisms involved.

The aim of the present study was, to get insight into the protein/protein interaction of ICln based on the structure of its water soluble form, which seems to connect multiple and different regulatory modules, a concept common for 'connector hubs' in complex protein-networks (3).

Here, we show the NMR solution structure of $ICln_{159}$, which demonstrates that ICln belongs to the pleckstrin homology (PH) domain superfold family of proteins.

PH-domains are highly conserved in regulatory proteins involved in intracellular signaling. The best characterized physiological role of PH-domains is to recruit and tether their host proteins to the cell membrane (27). PH-domains are also known as substrates for different kinases (27). Indeed, it was shown that ICln can be phosphorylated by a CKI/CKII like kinase (28). Sequence analysis predicts that ICln could also be phosphorylated by PKC, PKA, and PKGI or II. Here we show that $ICln_{159}$ interacts with PKC, PKA and, in addition, with PKGII, but not PKGI.

The finding that $ICln_{159}$ interacts with LSm proteins as well as kinases, suggests that the ICln PH-domain may serve as 'connector-hub'.

MATERIAL AND METHODS

Cloning - Starting from human (*Homo sapiens*) and dog (*Canis canis*) cDNA, the open reading frames of full length LSm4, ICln as well as of the different ICln truncations were amplified by PCR using standard protocols. The PCR products were cloned in frame into the mammalian expression vectors pECFP-C1, pEYFP-C1, pECFP-N1, pEYFP-N1 (Clontech, USA) to produce fusion proteins suitable for FRET. For protein purification, ICln and ICln truncations as well as LSm4 were cloned into the bacterial expression vector pET3-His (23). The primer pairs and restriction sites used for amplification and cloning are given in the supplement.

Protein expression - All proteins were expressed as N-terminal His6-tagged fusion proteins in *E. coli* BL21 (DE3) or BL21(DE3) pLys, grown in either minimal (29) or LB medium at 37 °C. Protein expression was induced by adding IPTG to the culture medium at an OD_{600} of 0.8. Bacteria were harvested by centrifugation two to four hours after induction of protein expression. Bacterial pellets of 1l of culture were resuspended in 30 ml of lysis buffer (ICln and ICln-truncations: 25mM K_2HPO_4, 200mM NaCl, 10 mM Imidazole-HCl, 5% glycerol, pH 7.2; LSm4: 25mM K_2HPO_4, 900mM NaCl, 1mM DTT, 5%

glycerol, pH 7.2) and lysed twice in a French press at 15000 psi.

Protein purification - Purification and labeling of ICln and its truncations in *E. coli* BL21(DE3) for NMR, interaction- and bilayer-experiments is described in detail in (23,25,29). For the purification of hsLSm4, bacterial lysates were cleared by centrifugation and loaded onto a cation exchange column (bed volume 8ml, MacroPrep High S, BioRad, Austria). After washing with 1M NaCl in 25mM K_2HPO_4, 1mM DTT, 5% glycerol, pH 7.2, bound proteins were eluted by increasing NaCl to 2M. Fractions containing LSm4 were pooled, concentrated and applied to a Sephacryl S100 gel filtration column (bed volume 125 ml, BioRad, Austria) equilibrated with 25mM K_2HPO_4, 150mM NaCl, 1mM DTT, 5% glycerol, pH 7.2. Fractions containing LSm4 were pooled, concentrated and stored at -70 ^{o}C. Protein-protein interaction assays were performed in GFC equilibration buffer at 4°C.

Bilayer experiments - The experimental procedure used for the reconstitution of ICln in 'black' lipid bilayers was previously described in detail (23,25). For the lipid bilayer membrane, a mixture (1:1) of DiphPC and DMPC, 1% (w/v) lipids in n-decane were employed. After the membrane was formed and its stability assessed, $ICln_{159}$ (500 ng/ml) was added to the cis and trans chambers. The experiments were made at 28°C, in a symmetrical solution composed of 100mM KCl, 5 mM HEPES, pH 8.00. In order to determine the ion selectivity of reconstituted $ICln_{159}$, we chose a gradient for the ions employed that had a higher salt concentration in the trans chamber (150mM KCl, 5 mM HEPES, pH 8.00), and a lower concentration in the cis chamber (10mM KCl, 5 mM HEPES pH 8.00). The chloride gradient (ΔPDCl) was measured after each experiment and used to calculate the pK/pCl value according to the Goldman-Hodgkin-Katz equation. Reversal potentials were determined graphically by interpolation and were normalized to a gradient of 15 (23,25).

NMR analysis - NMR data were acquired at 298K on Varian Inova 800 MHz and 500 MHz spectrometers equipped with pulse field gradient triple resonance probes (H/N/C). The NMR sample conditions were 1mM protein, 25mM K_2HPO_4, 150mM NaCl in 90% H_2O, 10 % $^{2}H_2O$, pH 7.0. NMR data were processed and analyzed with NMRPipe (30) and NMRView (31). Backbone and sidechain signal assignments as well as relaxation experiments were obtained using standard triple resonance experiments (32). Three bond nitrogen-carbon ($^{3}JC\gamma N$) and carbonyl-carbon ($^{3}JC\gamma C$) couplings were measured by quantitative J methods (33,34). Three dimensional structures were generated by simulated annealing with the XPLOR-NIH package (35). NOE distance restraints were derived from 3D-$^{15}N/^{13}C$-NOESY-HSQC (150 ms) crosspeaks, which were classified into strong, medium, weak (1.8 - 2.2 Å|1.8 - 3.4Å|1.8 - 6Å). Hydrogen bonds within the α-helix and between adjacent β–strands were inferred from NOE patterns. Backbone torsion angle restraints were obtained from backbone secondary chemical shifts using the TALOS software package (36) and X1 restraints from experimental $^{3}JC\gamma N/^{3}JC\gamma C$ couplings. Geometric quality of the calculated structures was analyzed using PROCHECK-NMR (37).

In vitro phosphorylation - Full length and mutant ICln (1μg/assay) were phosphorylated in vitro using purified catalytic subunit of cAMP-dependent protein kinase (PKA), purified protein kinase C (PKC; both purchased from Promega) and recombinant His-tagged human cGMP-dependent protein kinase type Iβ or II (PKGI or II) in a buffer containing 20mM Tris/HCl (pH=7.4) and 10mM $MgCl_2$, supplemented with 0.5mM $CaCl_2$, 0.6 μg diolein and 6 μg phosphatidylserine (PKC), 2mM β-mercaptoethanol (PKA and PKGI or II) or 0.01% Triton X-100 and 20μM cGMP (PKGI or II). Phosphorylation was started by the addition of 5 μl ATP (final concentration 120μM) containing 1μCi [γ-^{32}P]ATP (Amersham, Netherlands) and terminated after 30 min (30° C) by the addition of SDS sample mix. Proteins were separated by SDS-PAGE.

Mass spectrometry - Samples were digested overnight at 37°C with two different enzymes. Digestion with Staphylococcus aureus V8 Protease (Boehringer Mannheim) was performed in a 25 mM sodium phosphate buffer (pH 7.8), and digestion with trypsin (Roche, sequencing grade) in a 10 mM NH_4HCO_3 buffer (pH 8.9). Protein digests were analysed using capillary HPLC connected on-line to a LCQ ion trap instrument (ThermoFinnigan, San Jose, CA) equipped

with a nanospray interface as published previously (38). The nanospray voltage was set at 1.6 kV and the heated capillary was held at 170°C. MS/MS spectra were searched against the MDCK ICln sequence using TurboSEQUEST(BioWorks; ThermoFinnigan) with subsequent manual validation. Phosphorylation (+ 80 Da) was searched on serine, threonine and tyrosine residues as variable modification.

Whole cell patch-clamp in NIH3T3 fibroblasts - Whole cell patch-clamp measurements were made as described in detail by Gschwentner et al. (17,39). The isotonic extracellular solution used was (in mM): NaCl 125, $CaCl_2$ 2.5, $MgCl_2$ 2.5, HEPES 10, mannitol 50, pH 7.2 (adjusted with NaOH). To reduce extracellular osmolality, mannitol was omitted. The filling solution of the patch pipette was (in mM): CsCl 125, $MgCl_2$ 5, EGTA 11, raffinose 50, HEPES 10, ATP 2, cGMP 10µM, pH 7.2 (adjusted with CsOH).

FRET - FRET and acceptor photobleaching techniques as well as the NFRET calculations employed in this study are described in detail in Ritter et al. (20).

Salts, chemicals and drugs - All salts and chemicals were of p.a. grade. Lipids were purchased from Avanti Polar Lipids (USA).

Statistical analysis - All values are given as mean ± sem (sd in table1 – suppl.). Data were tested for differences in the means by Student's t-test after verifying normal distribution and equal variance within the data sets. A statistically significant difference was assumed at $p<0.05$.

RESULTS

The NMR structure of ICln - As shown in figure 1, the full length ICln protein from MDCK cells consists of 235 amino acids (AA) (1). Since this protein is prone to degradation (within days at RT) we decided to modify ICln by C-terminal truncation to circumvent problems with proteolysis during NMR data acquisition. Deleting the C-terminal 76 AA leads to a ICln protein comprised of the N-terminal 159 AA, which contains the putative transmembrane β-strands (1). This truncated form of ICln ($ICln_{159}$) proved to be very stable (for more than 1 week at RT), is monomeric in solution, and forms functional ion channels in lipid bilayers with a pK/pCl of 21.87 ± 4.2 (n=12). The selectivity of these channels can - similar to full length ICln - be shifted towards chloride after the addition of 2mM Ca^{2+} (pK/pCl = 7.86 ± 1.6; n=7; suppl. 1).

The NMR structure of $ICln_{159}$ exhibits a PH-domain topology. It consists, as shown in Fig. 2a, of a pair of nearly orthogonal anti-parallel β-sheets with strands β_2, β_3, and β_4 forming one, and strands β_1, β_5, β_6, and β_7 forming the other side of the β-barrel (suppl., table1). Near the C-terminus, the β–barrel is capped by a α-helix that is formed by residues 126-142. The loops between β_5 and β_6 as well as β_6 and β_7 are highly mobile as evidenced by little or no deviation of their shifts from random coil values and the high ^{15}N T_2 values of the amides (Fig. 2b).

The comparison of the HSQC spectra of $ICln_{159}$ and a deletion mutant of $ICln_{159}$ ($ICln_{\Delta loop}$) where 15 AA's (GLU89 – ASP103 = Δloop; Fig. 1) from the β_6-β_7 loop were deleted, leaving 8 AA's (ALA84, LYS85, PHE86, GLY87, GLU88 -Δ_{loop} – VAL104, GLU105, PRO106) to connect the strands β_6 and β_7, demonstrates no structural consequences on the β–barrel (suppl. 2). $ICln_{159}$ displays a very strong, overall negative electrostatic surface potential and shares this feature with the PH-domain of nematode UNC-89 (Fig. 3a, b).

Phosphorylation of ICln by PKA, PKC and PKGII – In platelets, pleckstrin, the archetypical PH-domain protein, is the main substrate for protein kinase C (PKC). As shown in Fig. 1, the sequence of ICln contains several putative phosphorylation sites for PKC, PKA, and PKGI or II. Phosphorylation by a CKI/II-like-kinase was shown by Sanchez-Olea and coworkers (28), and discussed as a potential regulatory mechanism (40).

Here we show that ICln can be phosphorylated by PKA, PKC and PKGII, but not by PKGI (Fig 4a). In order to pin down possible phosphorylation sites, we selectively mutated SER45 (exchanging serine by alanine; S45A) in ICln and the results are summarized in Fig. 4b. In $ICln_{S45A}$ phosphorylation by PKA is abolished and phosphorylation by either, PKC or PKGII is markedly reduced, demonstrating that SER45 is the sole target for PKA and the prime target for PKC as well as PKGII. The serine 45 is located in the β_3-strand of the ICln PH-domain (fig. 1). In order to identify further phosphorylation sites of

PKGII within the ICln PH-domain, we subjected PKGII phosphorylated $ICln_{159}$ to mass-spectrometry. We searched for peptides that differ by 80 mass units (mass of a single phosphate group), and by doing so, we identified S2 and S93 as additional PKGII phosphorylation sites of $ICln_{159}$. Interestingly, S93 is located within the mobile loop between strands β_6 and β_7 of the ICln PH-domain. No threonine or tyrosine phosphorylation was detected.

PKGII decreases RVD-channel (RVDC) activity – Regulatory volume decrease (RVD) is one of the functional modules in which ICln is involved. Since kinases (PKA and PKC) are able to modulate RVDC (41), we tested whether PKGII is also able to modulate endogenous RVDC. RVDC activity was measured in 3T3-NIH fibroblasts after reducing the extracellular osmolality by 50 mosM. This maneuver leads to an increase of RVDC currents from 0.03±0.01 nA (n=9) to 1.04±0.19 nA (n=9) at a holding potential of +40 mV (suppl. 4). In order to measure the effect of PKGII on RVDC we over-expressed PKGII in fibroblasts, and tested the PKGII effect - after activation with cGMP - on the endogenous RVDC. The baseline transcription of PKGII in fibroblasts is very low and fibroblasts are not the prime target for PKGII action (42). PKGII is primarily expressed in cells of the intestinal mucosa, brain as well as epithelial cells in the kidney (42). For the over-expression of PKGII we used an IRES-construct, which allows the simultaneous expression of PKGII and GFP (as a transfection marker) as two separate proteins. The expression of GFP alone did not significantly alter RVDC currents (from 0.11±0.04 nA (n=9; ISO) to 0.91±0.19 nA (n=9; HYPO); suppl. 4). The expression of PKGII however, abolishes inward currents of endogenous RVDC and markedly attenuates currents in the outward direction (reduction from 0.91±0.19 nA (n=9) to 0.33±0.06 nA (n=9)), without altering the currents under isotonic conditions (Fig. 5).

As described earlier, ICln is a substrate for PKGII, however, the reduced activity of RVDC followed by the expression and activation of PKGII could also be the result of the phosphorylation of a protein not related to ICln. In order to test for this hypothesis we tried to determine the phosphorylation of ICln in PKGII expressing cells. We were not able to detect phosphorylated ICln under these conditions (data not shown), most likely because the membrane fraction of ICln is, as reported, very small (5), and therefore the expected fraction of PKGII phosphorylated ICln probably below the sensitivity of our assay. Therefore, we used another approach to test if ICln is able to interact with PKGII under *in vivo* conditions. As shown in figure 5b, ICln and PKGII indeed interact at the level of the cell membrane, as evidenced by the specific FRET-signal, which amounts to 1.72 ± 0.15 NFRET (n=21), a value significantly (p=0.003) higher compared to the control value of 0.98 ± 0.17 NFRET (n=17), suggesting interaction of PKGII with endogenous ICln.

ICln binds to LSm4, a component of the splicing and RNA degradation machinery - Using the yeast-two-hybrid-system, we were able to identify ICln partner proteins involved in another functional module, namely RNA-splicing, i.e. Sm proteins (B/B', D1, D2, D3) as well as LSm proteins (LSm2 (SmX) and LSm4) ((10), and data not shown). Here we show that ICln as well as $ICln_{159}$ are able to bind to LSm4 in vitro (Fig. 6a-e).

The LSm4 protein has a molecular weight of 16.5kD and a calculated pI of 10.12, and is thus positively charged at physiological pH. In native PAGE, purified LSm4 does therefore not migrate into the gel. Consequently, LSm4 can only migrate into the gel, if it forms a complex with purified $ICln_{159}$ (Fig. 6b, lane 1) or full length ICln (Fig. 6b, lane 3), both of which are negatively charged (pI 4.17 and pI 4.05, resp.) and thus able to enter the gel and migrate towards the anode (Fig 6b, lanes 2 and 4). The results obtained with native PAGE were verified by gel filtration chromatography (GFC; Fig. 6a,c and e) and Western blotting (not shown) using LSm4 specific antibodies.

The interaction between ICln and LSm4 observed *in vitro,* was also tested under *in vivo* conditions. For these experiments, fusion proteins of LSm4 and ICln with ECFP as well as EYFP were constructed for fluorescence resonance energy transfer (FRET) measurements. For these experiments the donor-ECFP protein was fused to the N-terminus of ICln (ECFP-ICln) and the acceptor-EYFP protein fused to the N-terminus of LSm4 (EYFP-LSm4). In HEK293T cells

co-transfected with ECFP-ICln and EYFP-LSm4, acceptor (EYFP-LSm4) photo-bleaching leads to an increase in donor (ECFP-ICln) fluorescence, demonstrating FRET and hence interaction between ICln and LSm4 in living cells (Fig. 6f). FRET can be detected in the cytosol and in the immediate vicinity of the cell membrane (Fig 6f, inset). Exchanging donor and acceptor on the respective proteins did not alter the result in quantity and quality (Fig. 6f). However, fusing the fluorescing proteins (donor and acceptor) to the C-termini of ICln, or both LSm4 and ICln, annihilated the FRET signal (Fig. 6f).

In order to identify the binding site for LSm4 on ICln, we performed gel filtration chromatography and native PAGE using LSm4 and two different ICln mutants. As shown in figure 6c and d using the $ICln_{\Delta loop}$ mutant did not prevent complex formation, however, deleting further C-terminal 25 AA's from $ICln_{159}$, leading to $ICln_{134}$, did prevent LSm4 complex formation, suggesting that these 25 AA's comprise the binding site for LSm4 (Fig. 6d).

DISCUSSION

ICln is a multifunctional protein involved in several different regulatory modules within the living cell. Ion transport is one of these modules, since ICln is able to form ion channels by directly inserting from its water soluble form into the lipid membrane. Such a mode for channel insertion is well known for water-soluble bacterial toxin-channels (43). Further functional modules are the regulation of RNA spicing by the interaction of ICln with splicing factors (6-8,10,40), and the regulation of the cytoskeleton by ICln (5,11-13). The ability of ICln to interact with more than one regulatory module suggests that the water soluble form of ICln acts as a 'connector hub' (3) for different regulatory mechanisms. The aim of the present study was to identify the structure of water soluble, i.e. the 'connector hub' form of ICln. Based on the structure of ICln, we aimed to identify binding sites for partner-proteins like LSm4, or phosphorylation sites of different kinases. This experimental framework provides an important guide post for further studies aimed to elucidate the regulation of protein-networks in which ICln is involved.

In this study we determined the structure of a deletion mutant of ICln, i.e. $ICln_{159}$, which is water soluble, able to form ion channels in lipid bilayers, binds to LSm4, and serves as a substrate for PKA, PKC, and PKGII. The reason for using $ICln_{159}$ was the instable nature of full length ICln when used for the NMR analysis.

$ICln_{159}$ folds in to a PH-domain like structure. PH-domains are a large family of structurally homologous protein domains of moderate to low sequence homology and are found in many proteins involved in signal transduction (44-46). The canonical structure of PH-domains is a core seven-stranded β-sandwich capped by a C-terminal α-helix, and three major inter-strand loops that could serve as putative binding sites for protein-protein interactions (46). As described here, the β_6-β_7 loop of ICln is particularly mobile and long, when compared to other PH-domains. Usually, this loop is built by 4-5 AA's. However, PH-domains tolerate large insertions without effect on the core structure, e.g. one of the two PH-motifs of phospholipase Cγ is split at the β_3–β_4 loop by three src homology (SH)-domains leading to an insertion of 258AA's (47). Accordingly, deletion of 15AA within the β_6-β_7 loop did not alter the structure of $ICln_{159}$, demonstrating that the length of the β_6-β_7 loop is not affecting the core structure.

Scrutinizing the AA-sequence of $ICln_{159}$ for possible sites of phosporylation and analyzing putative target serines and threonines for accessibility on the structural model reveals three sites of interest, *i.e.* THR34, SER45 and SER115. As shown by single point mutagenesis, SER45 is the main target for PKA, PKC as well as PKGII. It is noteworthy that in contrast to other substrates of PKGII *in vivo*, *i.e.* CFTR (48,49), ICln is able to discriminate between PKGI and PKGII *in vitro* (Fig. 4a). Three PKGII phosphorylation sites, S2, S45 and S93, were identified by single point mutagenesis or mass spectrometry. As shown in figure 4b, S45 is the main phosphorylation site for PKGII as well as PKC. Interestingly, S93 is located exactly within the mobile loop connecting strands β_6 and β_7, and preliminary experiments indicate that this loop is important for current formation in lipid bilayers (S. Dopinto & M. Paulmichl, unpublished results). Therefore it is intriguing to speculate that phosphorylation of

S93 could modulate the ICln induced current. This scenario is speculative, however, FRET experiments reported in this study suggest a interaction between ICln and PKGII at the cell membrane, *in vivo*. Additional experiments need to be done to clarify this issue.

$ICln_{159}$ binds to LSm4 which is most likely methylated by PRMT5 that also methylates Sm-proteins (9,50,51). PRMT5 possibly binds to AD3 at the C-terminus of ICln (51). The experiments summarized in this study show that the binding of ICln to LSm4 involves the second acidic domain (AD2; fig. 1) situated immediately after the capping α-helix of the ICln PH-domain, but not AD1, located in the β_6 - β_7-loop of the ICln PH-domain. It is interesting to note that within this acidic domain there is a serine at position 142, which is phosphorylated by cytosolic extracts (40). This phosphorylation may potentially regulate Sm/LSm binding to ICln. However, this hypothesis needs to be tested.

In conclusion, the water-soluble form of ICln is a PH-domain like structure with a overall negative surface potential. The protein is a potential target for PKA, PKC and PKGII phosphorylation, and binds strongly to LSm4, a positively charged protein that is part of the spliceosome and of the RNA degradation machinery. As summarized in figure 7, water soluble ICln acts as a protein-protein interaction platform involved in different regulatory modules, which is a key-feature of 'connector hubs' in complex protein networks (3). By solving the structure of $ICln_{159}$, by determining the binding site of ICln for LSm4, and by demonstrating that ICln can be phosphorylated by PKC, PKA and PKGII on S45 as well as S2 and S93 (PKGII), we provide a valuable guiding post for the systematic exploration of the involvement of ICln in such diverse regulatory mechanisms as cell volume regulation, splicing, RNA degradation and cytoskeletal reorganization.

FOOTNOTES

* We thank Simona Rodighiero from the CIMAINA facility, University of Milan for technical assistance (FRET). Furthermore, we would like to thank Karine Smans (Janssen Pharmaceutica, Beerse, Belgium) for donating the PKGIß and PKGII kinases, Marcel Edixhoven, Matthias König, Sabine Chwatal and Sonja Eichmüller for technical assistance, and Prof. Luhrmann, (Max Planck Institute of Biophysical Chemistry, Goettingen, Germany) for the LSm4 antibodies. The work was supported by the Austrian Science Foundation (P13041-med, P15578 and P17119-B05) and the Italian Science Foundation (MURST) to MP, MR, RK and JF.

REFERENCES

1. Paulmichl, M., Li, Y., Wickmann, K., Ackerman, M., Peralta, E., and Clapham, D. (1992) *Nature* **356**, 238-241
2. Furst, J., Gschwentner, M., Ritter, M., Botta, G., Jakab, M., Mayer, M., Garavaglia, L., Bazzini, C., Rodighiero, S., Meyer, G., Eichmuller, S., Woll, E., and Paulmichl, M. (2002) *Pflugers Arch* **444**(1-2), 1-25
3. Guimera, R., and Nunes Amaral, L. A. (2005) *Nature* **433**(7028), 895-900
4. Pu, W. T., Wickman, K., and Clapham, D. E. (2000) *J Biol Chem* **275**(17), 12363-12366
5. Krapivinsky, G. B., Ackerman, M. J., Gordon, E. A., Krapivinsky, L. D., and Clapham, D. E. (1994) *Cell* **76**(3), 439-448
6. Friesen, W. J., Paushkin, S., Wyce, A., Massenet, S., Pesiridis, G. S., Van Duyne, G., Rappsilber, J., Mann, M., and Dreyfuss, G. (2001) *Mol Cell Biol* **21**(24), 8289-8300
7. Friesen, W. J., Wyce, A., Paushkin, S., Abel, L., Rappsilber, J., Mann, M., and Dreyfuss, G. (2002) *J Biol Chem* **277**(10), 8243-8247
8. Meister, G., Eggert, C., Buhler, D., Brahms, H., Kambach, C., and Fischer, U. (2001) *Curr Biol* **11**(24), 1990-1994
9. Pu, W. T., Krapivinsky, G. B., Krapivinsky, L., and Clapham, D. E. (1999) *Mol Cell Biol* **19**, 4113-4120
10. Schmarda, A., Fresser, F., Gschwentner, M., Fürst, J., Ritter, M., Lang, F., and Paulmichl, M. (2001) *Cell Physiol Biochem* **11**, 55-60
11. Tang, C.-J. C., and Tang, T. K. (1998) *Blood* **92**, 1442-1447
12. Li, Y., Tao, G., Nagasawa, H., Tazawa, H., Kobayashi, A., Itoh, H., and Tashima, Y. (1999) *J Biochem (Tokyo)* **126**(4), 643-649
13. Schwarz, R. S., Rybicki, A. C., and Nagel, R. L. (1997) *Biochem. J.* **327**, 609-616
14. Larkin, D., Murphy, D., Reilly, D. F., Cahill, M., Sattler, E., Harriott, P., Cahill, D. J., and Moran, N. (2004) *J Biol Chem* **279**(26), 27286-27293
15. Furst, J., Jakab, M., Konig, M., Ritter, M., Gschwentner, M., Rudzki, J., Danzl, J., Mayer, M., Burtscher, C. M., Schirmer, J., Maier, B., Nairz, M., Chwatal, S., and Paulmichl, M. (2000) *Cell Physiol Biochem* **10**(5-6), 329-334
16. Okada, Y. (1997) *Am J Physiol* **273**, C755-C789
17. Gschwentner, M., Nagl, O. U., Wöll, E., Schmarda, A., Ritter, M., and Paulmichl, M. (1995) *Pflügers Arch* **430**, 464-470
18. Chen, L., Wang, L., and Jacob, T. (1999) *Am J Physiol* **276**, C182-C192
19. Hubert, M., Levitan, I., Hoffman, M., Zraggen, M., ME, H., and Garber, S. (2000) *Biochim Biophys Acta* **1466**, 105-114
20. Ritter, M., Ravasio, A., Jakab, M., Chwatal, S., Furst, J., Laich, A., Gschwentner, M., Signorelli, S., Burtscher, C., Eichmuller, S., and Paulmichl, M. (2003) *J Biol Chem* **278**, 50163-50174
21. Tao, G. Z., and Tashima, Y. (2000) *Peptides* **21**(4), 485-490
22. Tao, G.-Z., Komatsuda, A., Miura, A. B., Kobayashi, A., Itoh, H., and Tashima, Y. (1998) *Biochem Biophys Res Comm* **247**, 668-673
23. Fürst, J., Bazzini, C., Jakab, M., Meyer, G., König, M., Gschwentner, M., Ritter, M., Schmarda, A., Botta, G., Benz, R., Deetjen, P., and Paulmichl, M. (2000) *Pflügers Arch* **440**, 100-115
24. Garavaglia, M., Dopinto, S., Ritter, M., Furst, J., Saino, S., Guizzardi, F., Jakab, M., Bazzini, C., Vezzoli, V., Dossena, S., Rodighiero, S., Sironi, C., Botta, G., Meyer, G., Henderson, R. M., and Paulmichl, M. (2004) *Cell Physiol Biochem* **14**(4-6), 231-240
25. Garavaglia, M. L., Rodighiero, S., Bertocchi, C., Manfredi, R., Furst, J., Gschwentner, M., Ritter, M., Bazzini, C., Botta, G., Jakab, M., Meyer, G., and Paulmichl, M. (2002) *Pflugers Arch* **443**(5-6), 748-753
26. Li, C., Breton, S., Morrison, R., Cannon, C. L., Emma, F., Sanchez-Olea, R., Bear, C., and Strange, K. (1998) *J Gen Physiol* **112**, 727-736
27. Lemmon, M. A., and Ferguson, K. M. (2000) *Biochem J* **350 Pt 1**, 1-18

28. Sanchez-Olea, R., Emma, F., Coghlan, M., and Strange, K. (1998) *Biochim Biophys Acta* **1381**, 49-60
29. Schedlbauer, A., Kontaxis, G., Konig, M., Furst, J., Jakab, M., Ritter, M., Garavaglia, L., Botta, G., Meyer, G., Paulmichl, M., and Konrat, R. (2003) *J Biomol NMR* **27**(4), 399-400
30. Delaglio, F., Grzesiek, S., Vuister, G. W., Zhu, G., Pfeifer, J., and Bax, A. (1995) *J Biomol NMR* **6**(3), 277-293
31. Johnson, B., and Blevins, R. (1994) *J Biomol NMR* **4**, 603-614
32. Cavanagh, J., Fairbrother, W., Palmer, A., and Skelton, N. (1996) *Measurements of three bond nitrogen-carbon J couplings in proteins uniformly enriched in 15N and 13C*, Academic Press, INC, San Diego
33. Vuister, G., Wang, A., and Bax, A. (1993) *J Am Chem Soc* **115**, 5334-5335
34. Grzesiek, S., Vuister, G. W., and Bax, A. (1993) *J Biomol NMR* **3**(4), 487-493
35. Schwieters, C. D., and Clore, G. M. (2001) *J Magn Reson* **149**(2), 239-244
36. Cornilescu, G., Delaglio, F., and Bax, A. (1999) *J Biomol NMR* **13**(3), 289-302
37. Laskowski, R. A., Rullmannn, J. A., MacArthur, M. W., Kaptein, R., and Thornton, J. M. (1996) *J Biomol NMR* **8**(4), 477-486
38. Ott, H. W., Lindner, H., Sarg, B., Mueller-Holzner, E., Abendstein, B., Bergant, A., Fessler, S., Schwaerzler, P., Zeimet, A., Marth, C., and Illmensee, K. (2003) *Cancer Res* **63**(21), 7507-7514
39. Gschwentner, M., Susanna, A., Wöll, E., Ritter, M., Nagl, U. O., Schmarda, A., Laich, A., Pinggera, G. M., Ellemunter, H., Huemer, H., Deetjen, P., and Paulmichl, M. (1995) *Mol Med* **1**, 407-417
40. Grimmler, M., Bauer, L., Nousiainen, M., Korner, R., Meister, G., and Fischer, U. (2005) *EMBO Rep* **6**(1), 70-76
41. Jakab, M., Furst, J., Gschwentner, M., Botta, G., Garavaglia, M. L., Bazzini, C., Rodighiero, S., Meyer, G., Eichmueller, S., Woll, E., Chwatal, S., Ritter, M., and Paulmichl, M. (2002) *Cell Physiol Biochem* **12**(5-6), 235-258
42. Jarchau, T., Hausler, C., Markert, T., Pohler, D., Vanderkerckhove, J., De Jonge, H. R., Lohmann, S. M., and Walter, U. (1994) *Proc Natl Acad Sci U S A* **91**(20), 9426-9430
43. Lakey, J. H., Gonzalez-Manas, J. M., van der Goot, F. G., and Pattus, F. (1992) *FEBS Lett* **307**, 26-29
44. Musacchio, A., Gibson, T., Rice, P., Thompson, J., and Saraste, M. (1993) *Trends Biochem Sci* **18**(9), 343-348
45. Lemmon, M. A., Ferguson, K. M., and Abrams, C. S. (2002) *FEBS Lett* **513**(1), 71-76
46. Lemmon, M. A. (2004) *Biochem Soc Trans* **32**(Pt 5), 707-711
47. Sugimoto, K., Mori, Y., Makino, K., Ohkubo, K., and Morii, T. (2003) *J Am Chem Soc* **125**(17), 5000-5004
48. Vaandrager, A. B., Smolenski, A., Tilly, B. C., Houtsmuller, A. B., Ehlert, E. M., Bot, A. G., Edixhoven, M., Boomaars, W. E., Lohmann, S. M., and de Jonge, H. R. (1998) *Proc Natl Acad Sci U S A* **95**(4), 1466-1471
49. Ruth, P. (1999) *Pharmacol Ther* **82**(2-3), 355-372
50. Brahms, H., Meheus, L., de Brabandere, V., Fischer, U., and Luhrmann, R. (2001) *Rna* **7**(11), 1531-1542
51. Emma, F., Sanchez-Olea, R., and Strange, K. (1998) *Biochim Biophys Acta* **1404**, 321-328
52. Koradi, R., Billeter, M., and Wuthrich, K. (1996) *J Mol Graph* **14**(1), 51-55, 29-32
53. Jobin, C. M., Chen, H., Lin, A. J., Yacono, P. W., Igarashi, J., Michel, T., and Golan, D. E. (2003) *Biochemistry* **42**(40), 11716-11725

FIGURE LEGENDS

Fig. 1. AA sequence of ICln. In capital letters (single letter code) the AA's of full length ICln and the different truncations used (indicated by arrows) are given. The loop-deletion (Δloop) is indicated by a blue box. On top of the AA sequence, the secondary structure (β_1-β_7-strands and the α-helix) as determined by NMR, corresponding to the canonical PH-domains, is indicated. The four putative transmembrane β-strands described as the pore region of the ICln-channel (1) are indicated in green letters. The three acidic domains (AD1-3) are indicated by red boxes and labeled accordingly. The putative AA's phosphorylated by PKA, PKC and PKGI or II are given by large letters in red, and the respective kinases are indicated.

Fig. 2. NMR structure of water soluble $ICln_{159}$. (a) A bundle of 15 final structures and a ribbon plot of ICln were the β_6/β_7-loop is displayed in *magenta*, β-sheets in *cyan* and the α-helix in *red*. Only regions of regular secondary structure were best fitted relative to each other. (b) T_2 versus amino acid sequence of the backbone amide protons. The loop between strand β_6 and β_7 is disordered and highly mobile and indicated with a bar in *magenta*. *Green* columns indicate the β-sheets, the *gray* column indicates the α-helix. The numbering of the respective secondary structures is identical to figure 2a. The statistics for the final 15 ICln structures are given in the supplement, table1.

Fig. 3. Comparison of the electrostatic surface potential of (a) ICln with those of (b) UNC-89, and (c) β-spectrin (negatively charged AA's are given in red and positive in blue; the images were generated using MOLMOL (52).

Fig. 4. Phosphorylation of ICln. (a) Phosphorylation of purified ICln by PKA, PKC, PKGIβ and PKGII (16±2%, 41±2%, 4±1% and 100%, n=4, resp.). (b) Phosphorylation of ICln and $ICln_{S45A}$ by PKC, PKA and PKGII. The single point mutation in full length ICln leads to an 83% (n = 2) reduction of ICln phosphorylation by PKGII.

Fig. 5. (a) Whole cell patch clamp experiments using NIH3T3 fibroblasts expressing PKGII. In cells expressing PKGII, the endogenous swelling induced chloride current is significantly smaller when compared to cells expressing the GFP-marker protein alone (a summary of experiments comparing GFP expressing cells and cells treated solely by the transfection procedure is given in the suppl. 3). (b) Normalized FRET (NFRET) in NIH3T3 fibroblasts expressing either PKGII-CFP and YFP (control) or PKGII-CFP and YFP-hsICln.

Fig. 6. Interaction of ICln with LSm4. (a) Gel filtration chromatography; SDS-PAGE of peak fractions of purified LSm4-$ICln_{159}$ or LSm4-ICln complexes; lane 1: fraction of LSm4 control run collected at elution time of the $ICln_{159}$-LSm4 complex; lane 2: $ICln_{159}$-LSm4 complex; lane 3: ICln-LSm4 complex; lane 4: purified $ICln_{159}$; lane 5: purified ICln; lane 6: purified LSm4. (b) Native PAGE; lane 1: complex between $ICln_{159}$ and LSm4 is marked by an asterisk; lane 2: purified $ICln_{159}$; lane 3: complex between ICln and LSm4 is marked by an asterisk; lane 4: purified ICln. (c) Gel filtration chromatography; SDS-PAGE of peak fractions of purified LSm4-$ICln_{159\Delta loop}$ complexes; lane 1: fraction of LSm4 control run collected at elution time of the LSm4-$ICln_{159\Delta loop}$ complex; lane 2: $ICln_{159}$-LSm4 complex; lane 3: purified LSm4; lane 4: purified $ICln_{159\Delta loop}$. (d) Native PAGE; lane 1: purified $ICln_{159}$; lane 2: complex of $ICln_{159}$ and LSm4 is marked by an asterisk; lane 3: purified $ICln_{159\Delta loop}$; lane 4: complex of $ICln_{159\Delta loop}$ and LSm4 is marked by an asterisk; lane 5: purified $ICln_{134}$; lane 6: $ICln_{134}$ does not bind to LSm4. (e) Gel filtration chromatography; elution profiles of the $ICln_{159}$-LSm4 complex, $ICln_{159}$ or LSm4. (f) Interaction of ICln with LSm4 in vivo as determined by FRET. FRET efficiency was calculated according to Jobin et al. (53); I: ICln-ECFP/EYFP-LSm4 (n=7); II: ICln-ECFP/LSm4-EYFP (n=8); III: EYFP-ICln/ECFP-LSm4 (n=9); IV: ECFP-ICln/EYFP-LSm4 (n=5).

Fig. 7. ICln depicted as a hub, connecting different functional modules

Figures 1-4 final size:

Figure 1

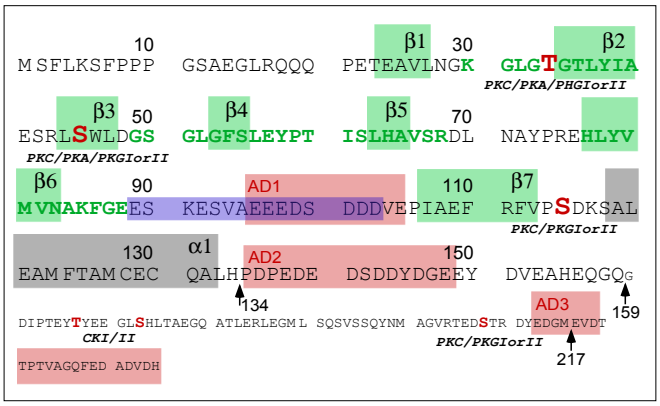

Figure 2

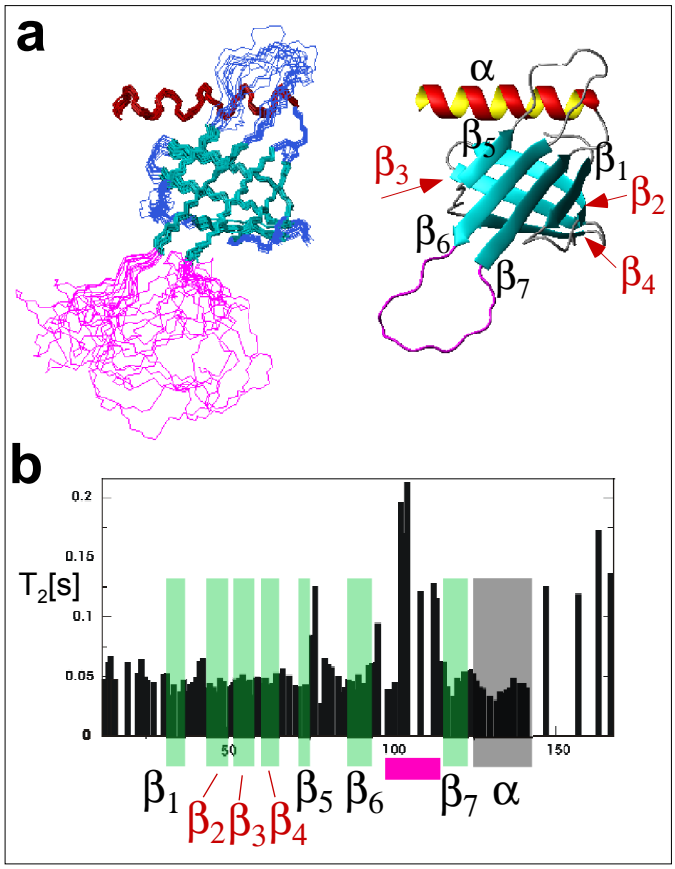

Figure 3

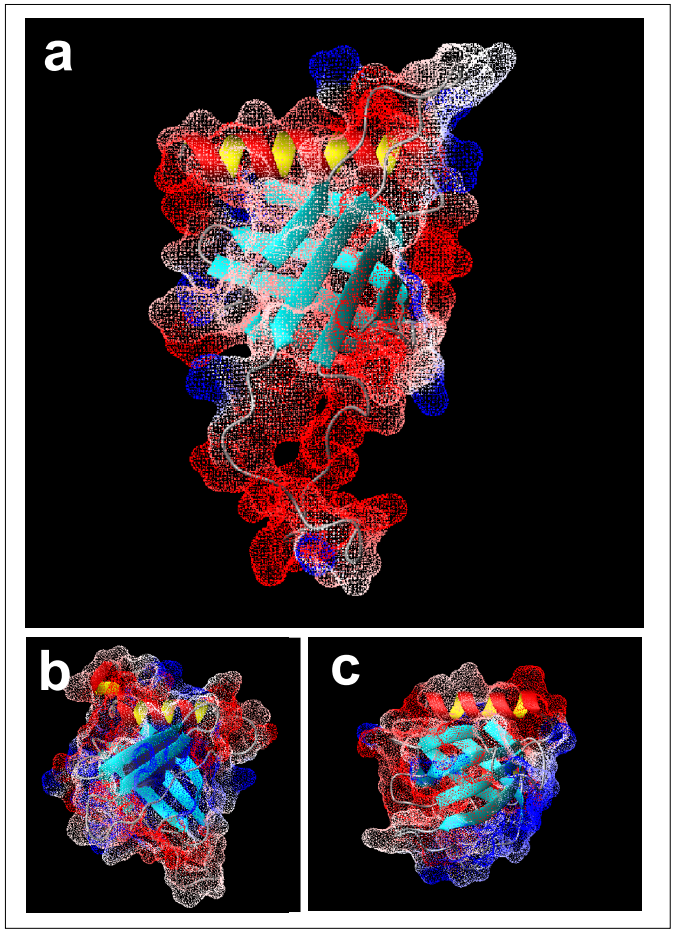

Figure 4

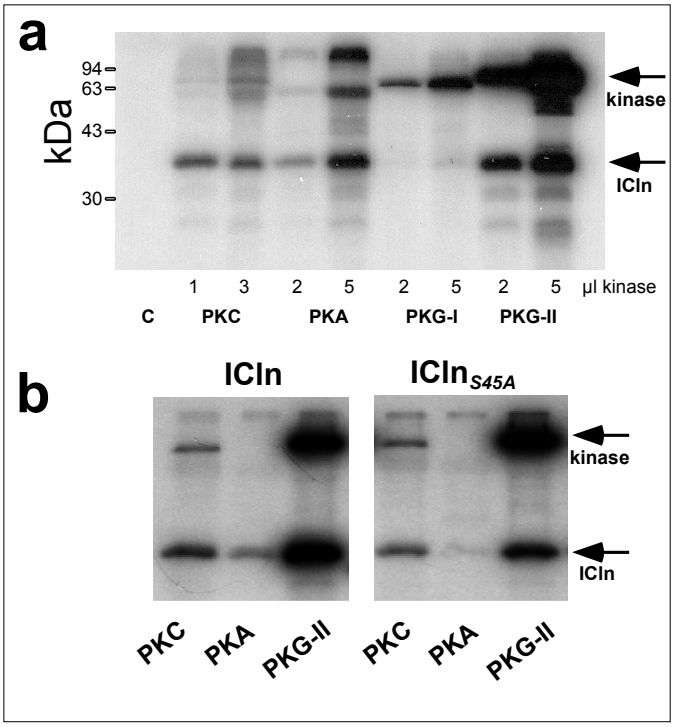

Figures 5-7 final size:

Figure 5

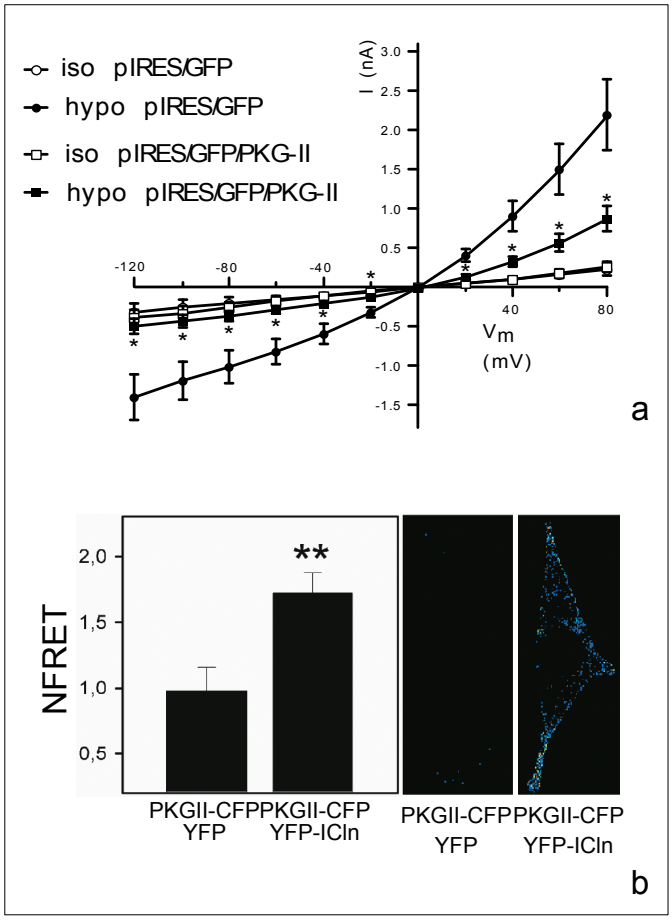

Figure 7

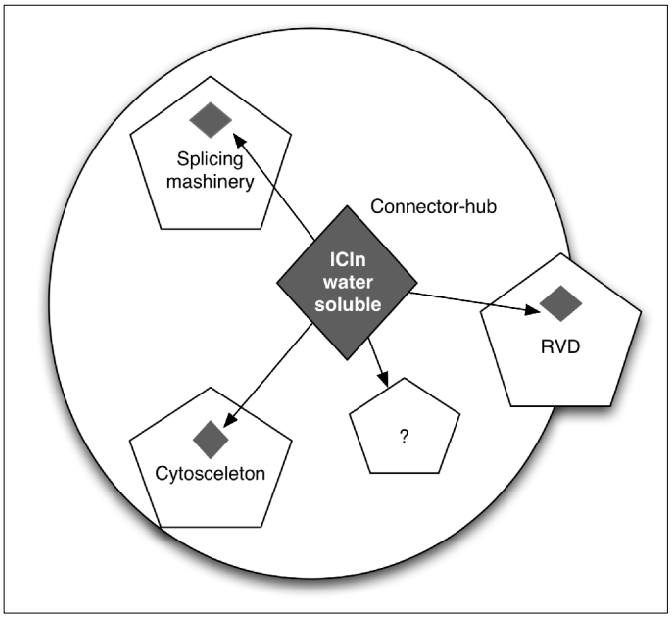

Figure 6

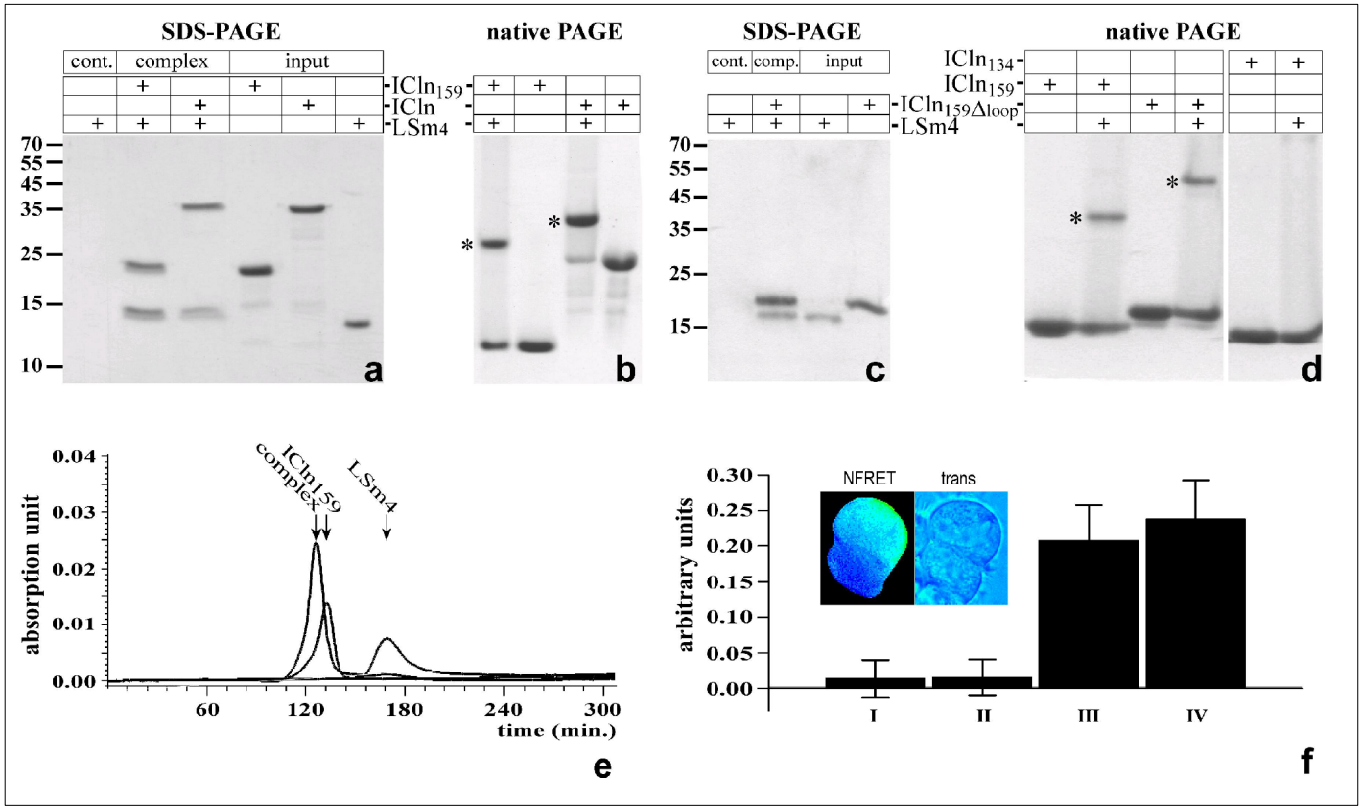

SUPPLEMENT

Material and Methods:

The following primer pairs and restriction sites (underlined) were used for amplification and cloning:

Mammalian expression (for FRET)
Vector: ECFP-N1, EYFP-N1, ECFP-C1 or EYFP-C1 (Clontech, USA):

hsICln (RE-sites Xho I; Bam HI)

hsICln-ECFP and hsICln-EYFP (ECFP-N1; EYFP-N1):

forward:	5' CGAATTCTCGAGATGAGCCTTCCTCAAAAGTTTCCCG 3'
reverse:	5' GGAATTCGGATCCGCGTGATCAACATCTGCATCCTCAAA 3'

ECFP-hsICln and EYFP-hsICln (ECFP-C1; EYFP-C1):

forward:	5' CGAATTCTCGAGGGATGAGCCTTCCTCAAAAGTTTCCCG 3'
reverse:	5' GGAATTCGGATCCTCAGTGATCAACATCTGCATCCT 3'

hsLSm4 (RE-sites Xho I, Kpn I)

hsLSm4-ECFP and hsLSm4-EYFP (ECFP-N1; EYFP-N1):

forward:	5' CCAGCTCGAGATGCTTCCCTTGTCACTGCTGA 3'
reverse:	5' CTCACGGTACCCCCTGTTTGCCCGCCTGTCTG 3'

ECFP-hsLSm4 and EYFP-hsLSm4 (ECFP-C1; EYFP-C1):

forward:	5' CCAGCTCGAGGACTTCCCTTGTCACTGCTGAA 3'
reverse:	5' CTCACGGTACCTCACTGTTTGCCCGCCTGTCT 3'

rat PKGII (RE-sites Xho I, Kpn I)

ratPKGII-ECFP (ECFP-N1)

forward:	5' CCAAGCTCGAGATGGGAAATGGTTCAGTGAAAC 3'
reverse:	5' AAGAGGGTACCTTGAAGTCCTTATCCCAGCCTG 3'

Bacterial expression
Vector: pET3-His (N-terminal H6-tag; (1) or pQE60 (C-terminal H6-tag, Qiagen, Germany)

ICln and ICln truncations
pET3-His; RE-sites Xho I, Bam HI

forward:	5' CGAATTCTCGAGATGAGCTTCCTCAAAAGTTTCCCG 3'
reverse:	
ccICln:	5' GGAATTCGGATCCTCAGTGATCAACATCTGCATCCT 3'
ccICln217:	5' CGAATTCGGATCCTCACTCCATCCCATCTTCATAAT 3'
ccICln159:	5' CGAATTCGGATCCTCACTGCCCTTGTTCATGTGCT 3'
ccICln134:	5' ACACAGGATCCTCAATGCAAGGCCTGGCATTC 3'

hsLSm4
Vector: pET3-His; RE-sites Xho I, Nco I

NMR:

TABLE 1

Structural statistics for the final 15 $ICln_{159}$ structures

Parameter	value
Distance restraints	
Total distance restraints:	959
Intraresidue:	203
Sequential backbone (|i-j|=1):	318
Interresidue, medium-range (4=<|i-j|=<2):	127
Interresidue, long-range (|i-j|>4):	311
Torsions restraints	
Backbone- φ,ψ -Torsions (TALOS):	174
X_1-Torsions ($^3J_{C\gamma N}/^3J_{C\gamma C'}$):	15
Hydrogen bonds:	48
Average rms-devations from experimental distance restraints:[Ă]:	0.092
Average rms-devations from idealized covalent geometry:	
Bonds[Ă]:	5.931E-03 +/- 1.271E-04
Angles[°]:	7.857E-01 +/- 2.059E-02
Improper[°]:	6.160E-01 +/- 2.311E-02
PROCHECK statistics	
Percentage residues in allowed regions of Ramachandran plot:	
Whole molecule	99.5%
Residues in ordered structure elements[a]	100%

Root mean square deviations form the mean structure calculated from the final ensemble of 15 structures of $ICln_{159}$

Selected residues	Selected atoms	RMSD
All elements of secondary structure	Backbone atoms	0.398
	All heavy atoms	0.774
	All atoms	0.943
Whole molecule except unstructured C- and N-Terminus[b]	Backbone atoms	3.318
	All heavy atoms	3.785
	All atoms	3.733
Whole molecule except loop β_6-ß$_7$, unstructured C- and N-Terminus[c]	Backbone atoms	0.762
	All heavy atoms	1.398
	All atoms	1.598

[a] statistic apply to ordered regions of ICln, with residues 33-36 (β_1), residues 44-49 (β_2), residues 53-56 (β_3), residues 62-64 (β_4), residues 72-74 (β_5), residues 86-92 (β_6), residues 116-122 (β_7), and residues 128-142 (α-helix).

[b] comprising residues 33-142.

[c] comprising residues 33-92 and residues 116-142.

Supplement figure legends:

Supplement 1:

Functional reconstitution of $ICln_{159}$ in lipid bilayers. Current/voltage (I/V) relationship of reconstituted $ICln_{159}$ in symmetrical (a) as well as asymmetrical KCl conditions (b). The reversal potential is shifted towards chloride after the addition of 2 mM calcium (b). In (c) the summary of the experiments in (b) is given. The presence of 2 mM calcium leads to less potassium selective ion currents (pK/pCl).

Supplement 2:

Assigned $^{1}H^{N}$-^{15}N HSQC spectra of $ICln_{159}$ (blue) and $ICln_{159\Delta loop}$ (red). Deletion of 15 AA's in the β_6-β_7 loop does not affect the structure of $ICln_{159}$.

Supplement 3:

Whole cell patch plamp experiments on native NIH3T3 fibroblasts, and fibroblasts expressing GFP. The expression of GFP does not alter the swelling induced chloride current.

References:

1. Fürst, J., Bazzini, C., Jakab, M., Meyer, G., König, M., Gschwentner, M., Ritter, M., Schmarda, A., Botta, G., Benz, R., Deetjen, P., and Paulmichl, M. (2000) *Pflügers Arch* **440**, 100-115

Supplement (Fürst et al.):

Supplement 1

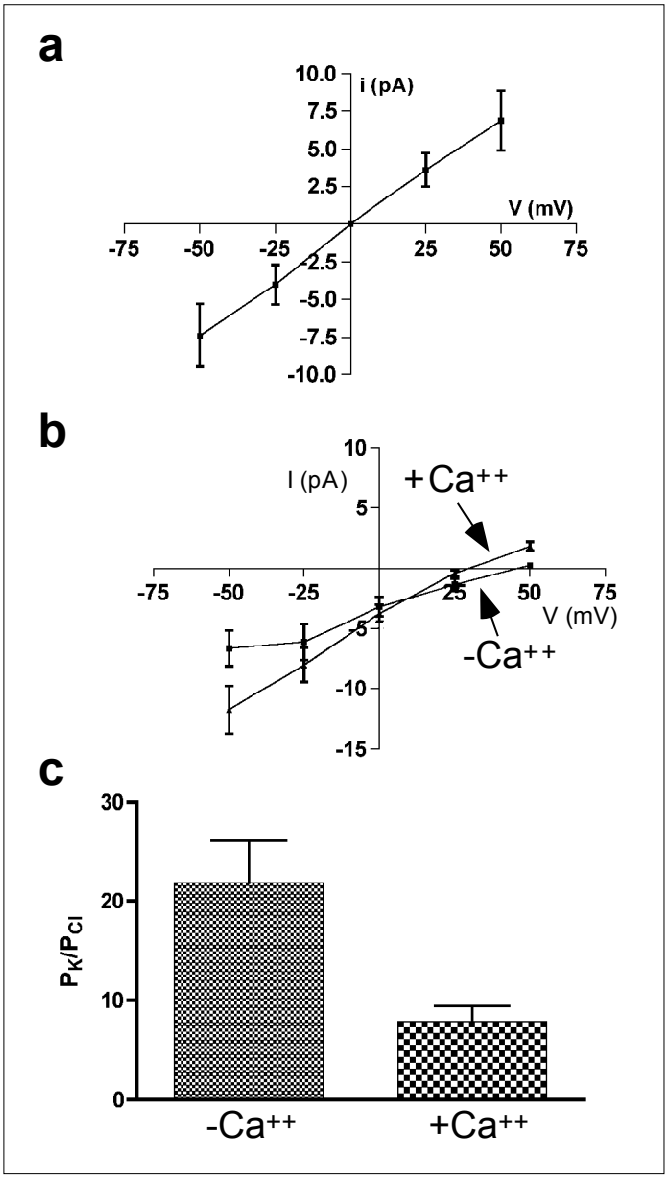

Supplement 3

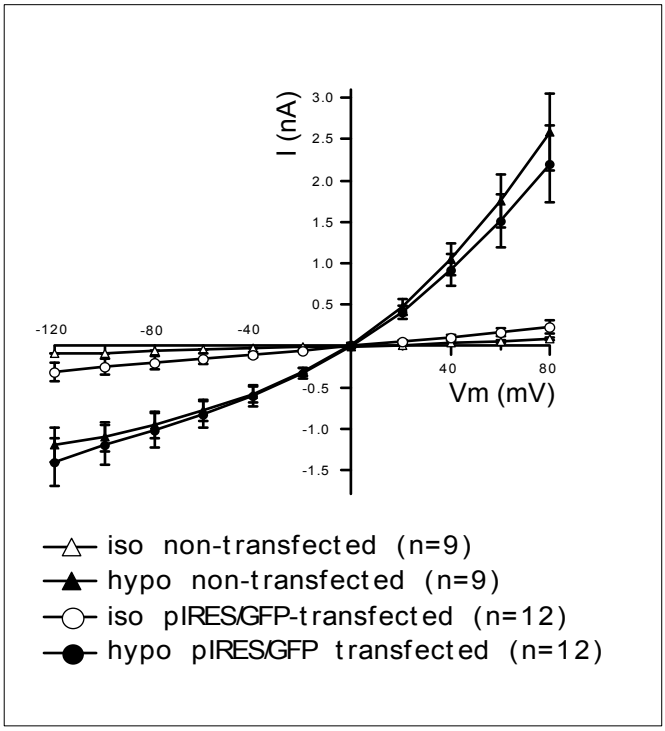

Supplement 2

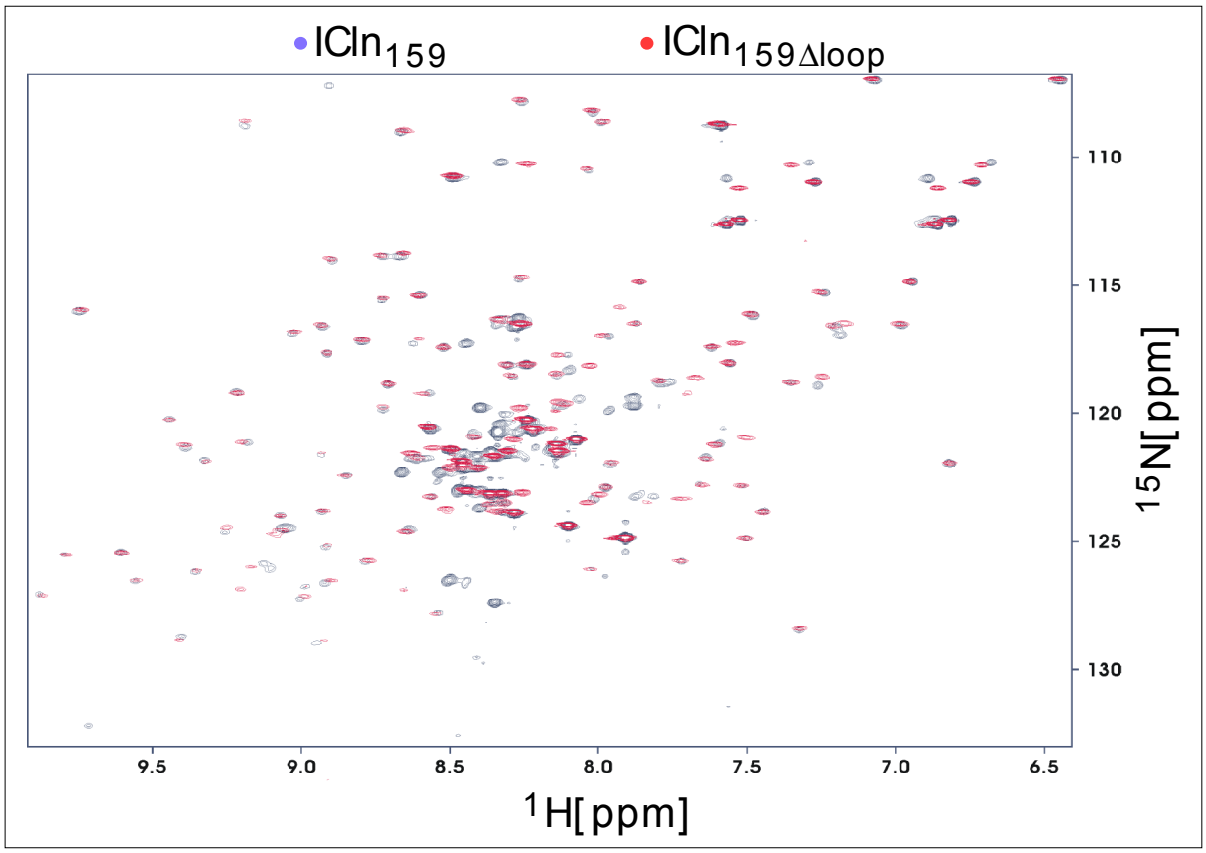

ICln159 folds into a PH-domain like structure: Interaction with kinases and the splicing-factor LSm4

Johannes Fürst, Andreas Schedlbauer, Rosaria Gandini, Maria Lisa Garavaglia, Stefano Saino, Martin Gschwentner, Bettina Sarg, Herbert Lindner, Martin Jakab, Markus Ritter, Claudia Bazzini, Guido Botta, Giuliano Meyer, Georg Kontaxis, Ben C. Tilly, Robert Konrat and Markus Paulmichl

J. Biol. Chem. published online May 19, 2005
